Supplemental Document

Biomedical Optics EXPRESS

Attention mechanism-based locally connected network for accurate and stable reconstruction in Cerenkov luminescence tomography: supplement

XIAONING ZHANG,[1,2,5] MEISHAN CAI,[2,3,5] LISHUANG GUO,[1,2] ZEYU ZHANG,[1,2] BILUO SHEN,[2,3] XIAOJUN ZHANG,[4] ZHENHUA HU,[2,3,6] AND JIE TIAN[1,2,3,7]

[1] *Beijing Advanced Innovation Center for Big Data-Based Precision Medicine, School of Medicine, Beihang University, Beijing, China*
[2] *CAS Key Laboratory of Molecular Imaging, Beijing Key Laboratory of Molecular Imaging, The State Key Laboratory of Management and Control for Complex Systems, Institute of Automation, Chinese Academy of Sciences, Beijing, China*
[3] *School of Artificial Intelligence, University of Chinese Academy of Sciences, Beijing, China*
[4] *Department of Nuclear Medicine, Chinese PLA General Hospital, Beijing, 100853, China*
[5] *Equal contribution*
[6] *zhenhua.hu@ia.ac.cn*
[7] *tian@ieee.org*

Supplement DOI: https://doi.org/10.6084/m9.figshare.16982074

Parent Article DOI: https://doi.org/10.1364/BOE.443517

Attention mechanism based locally connected network for accurate and stable reconstruction in Cerenkov luminescence tomography: supplemental document

1. The Experimental Process

This section illustrates the procedure of CLT reconstruction based on AMLC network. As shown in Fig.S1, the major steps are as follows:

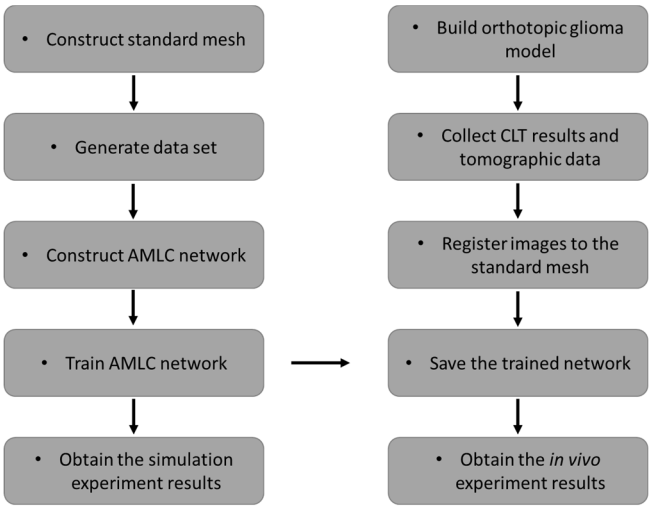

Fig.S1. The research flow diagram.

Step 1: Establish the standard meshes based on the mouse head CT data.

Step 2: Generate numerous single-source (5000 samples in our experiment) and big-source samples (8 times larger than single-source) using Monte Carlo simulation (MOSE v2.3). Dual-source samples are assembled randomly from single sources. 14,800 samples were finally generated in our experiments.

Step 3: Construct AMLC network, which contains four fully connected (FC) sub-network and five locally connected (LC) sub-network.

Step 4: Train AMLC network. The mean square error is adopted as the loss function. The Adam algorithm is considered as the optimizer function. All these samples gained from Step 2 are shuffled and sent into the network for training.

Step 5: Adjust the training parameters to converge the network training process. The trained network weights are saved for CLT reconstruction and the simulation experiment results are obtained.

Step 6: Build the tumor model with glioma cell line U87MG-Luc-GFP.

Step 7: Collect *in vivo* BLI, CLI, PET and MRI information.

Step 8: Register CLI results to the surface of the standard mesh.

Step 9: Obtain the *in vivo* CLI reconstruction results.

2. Depth Experiment

This section presents the reconstruction results of depth experiment. Three samples of different depths were shown in Fig. S2. The center distance between each sample was 1mm.

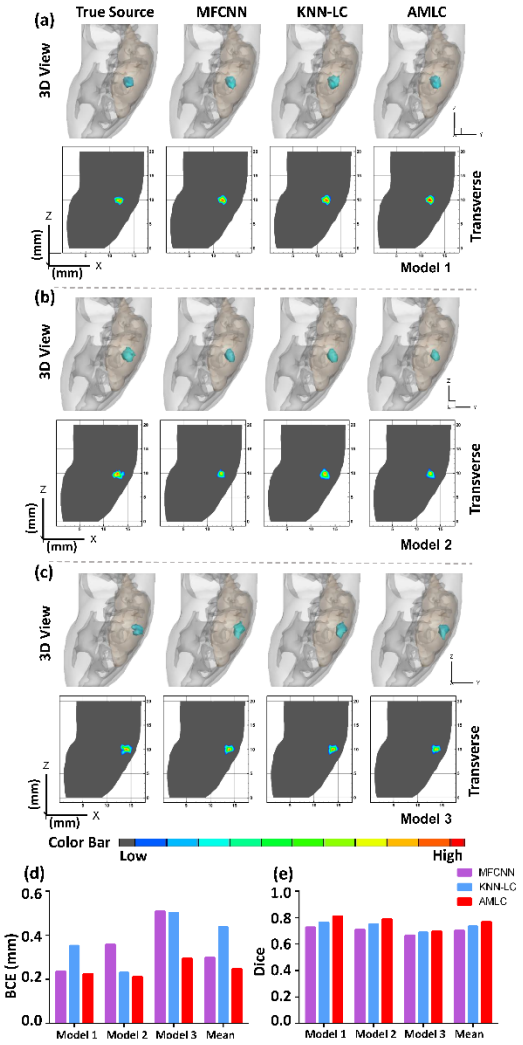

Fig.S2. CLT reconstruction results of depth experiment. (a-c) show the 3D views and 2D cross sections in different depth. (d) represents BCE in different depth, while (e) stands for Dice of reconstructed sources.

All three networks had achieved different depths of tumor reconstruction. However, the performance of MFCNN was not stable. The closer the tumor was to the surface, the worse the reconstruction effect of MFCNN was. Besides, KNN-LC network had advantages in

morphological restoration, but BCE results were not satisfactory. In general, AMLC network had obtained superior results at different depths with its small BCE.

3. Dual-source Reconstruction

As shown in Fig. S3, three samples were selected to show dual-source reconstruction results. All the results revealed accurate source locations. Due to the complexity of the dual-source, the morphological restoration was unsatisfactory. AMLC network still achieved relatively better performance in model 4 and model 5 in 3D view. Unexpected artifacts were observed in MFCNN result in model 5. However, AMLC network result in model 4 with rather small BCE achieved more accurate morphology recovery in both 3D view and 2D cross sections. These results demonstrated the superiority of AMLC network for complex source reconstruction.

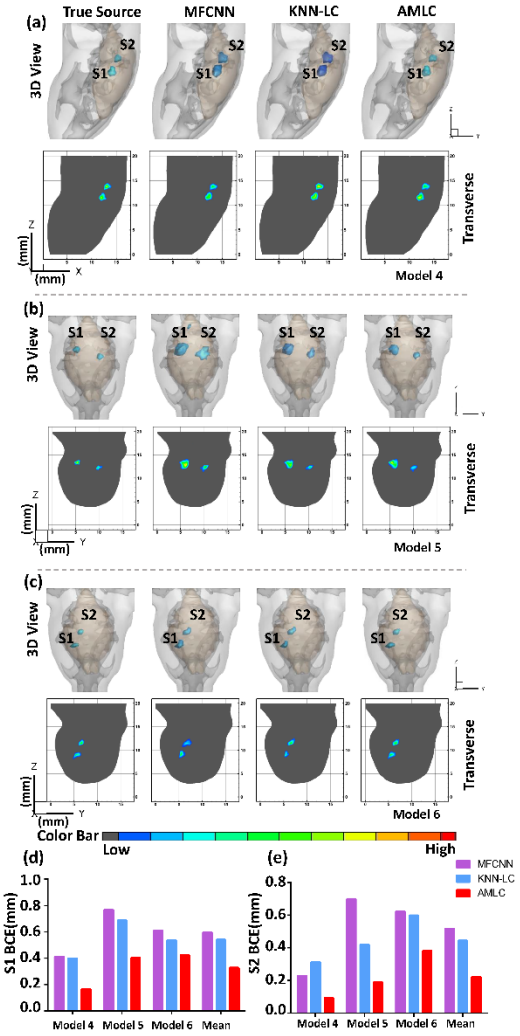

Fig. S3. CLT reconstruction results of dual-source. (a-c) show the real and reconstructed sources in different methods, respectively. Both 3D views and 2D cross sections were demonstrated. Quantitative analysis was shown in (d-e). (d-e) represent S1 BCE and S2 BCE, respectively.